Mutations in *AGBL5*, Encoding α-Tubulin Deglutamylase, Are Associated With Autosomal Recessive Retinitis Pigmentosa

Galuh D. N. Astuti,[1–3] Gavin Arno,[4] Sarah Hull,[4] Laurence Pierrache,[5–8] Hanka Venselaar,[9] Keren Carss,[10,11] F. Lucy Raymond,[11,12] Rob W. J. Collin,[1,13] Sultana M. H. Faradz,[3] L. Ingeborgh van den Born,[5] Andrew R. Webster,[4] and Frans P. M. Cremers[1,13]

[1]Department of Human Genetics, Radboud University Medical Center, Nijmegen, The Netherlands
[2]Radboud Institute for Molecular Life Sciences, Radboud University, Nijmegen, The Netherlands
[3]Division of Human Genetics, Center for Biomedical Research, Faculty of Medicine, Diponegoro University, Semarang, Indonesia
[4]University College London, Institute of Ophthalmology, London, United Kingdom
[5]The Rotterdam Eye Hospital, Rotterdam, The Netherlands
[6]Rotterdam Ophthalmic Institute, Rotterdam, The Netherlands
[7]Department of Ophthalmology, Erasmus Medical Center, Rotterdam, The Netherlands
[8]Department of Epidemiology, Erasmus Medical Center, Rotterdam, The Netherlands
[9]Centre for Molecular and Biomolecular Informatics, Radboud University, Nijmegen, The Netherlands
[10]Department of Haematology, University of Cambridge, Cambridge, United Kingdom
[11]National Institute for Health Research England BioResource–Rare Diseases, Cambridge University Hospitals, Cambridge Biomedical Campus, Cambridge, United Kingdom
[12]Department of Medical Genetics, Cambridge Institute for Medical Research, University of Cambridge, Cambridge, United Kingdom
[13]Donders Institute for Brain, Cognition and Behaviour, Radboud University Nijmegen, The Netherlands

Correspondence: Frans P. M. Cremers, Department of Human Genetics, Radboud University Medical Center, P.O. Box 9101, 6500 HB, Nijmegen, The Netherlands; Frans.Cremers@radboudumc.nl.

LIVDB, ARW, and FPMC are joint senior authors.

GDNA, GA, and SH contributed equally to the work presented here and should therefore be regarded as equivalent authors.

Submitted: June 19, 2016
Accepted: October 10, 2016

Citation: Astuti GDN, Arno G, Hull S, et al. Mutations in *AGBL5*, encoding α-tubulin deglutamylase, are associated with autosomal recessive retinitis pigmentosa. *Invest Ophthalmol Vis Sci*. 2016;57:6180–6187. DOI:10.1167/iovs.16-20148

Purpose. *AGBL5*, encoding ATP/GTP binding protein-like 5, was previously proposed as an autosomal recessive retinitis pigmentosa (arRP) candidate gene based on the identification of missense variants in two families. In this study, we performed next-generation sequencing to reveal additional RP cases with *AGBL5* variants, including protein-truncating variants.

Methods. Whole-genome sequencing (WGS) or whole-exome sequencing (WES) was performed in three probands. Subsequent Sanger sequencing and segregation analysis were performed in the selected candidate genes. The medical history of individuals carrying *AGBL5* variants was reviewed and additional ophthalmic examinations were performed, including fundus photography, fundus autofluorescence imaging, and optical coherence tomography.

Results. *AGBL5* variants were identified in three unrelated arRP families, comprising homozygous variants in family 1 (c.1775G>A:p.(Trp592*)) and family 2 (complex allele: c.[323C>G; 2659T>C]; p.[(Pro108Arg; *887Argext*1)]), and compound heterozygous variants (c.752T>G:p.(Val251Gly) and c.1504dupG:p.(Ala502Glyfs*15)) in family 3. All affected individuals displayed typical RP phenotypes.

Conclusions. Our study convincingly shows that variants in *AGBL5* are associated with arRP. The identification of *AGBL5* and *TTLL5*, a previously described RP-associated gene encoding the tubulin tyrosine ligase-like family, member 5 protein, highlights the importance of poly- and deglutamylation in retinal homeostasis. Further studies are required to investigate the underlying disease mechanism associated with *AGBL5* variants.

Keywords: retinitis pigmentosa, whole exome sequencing, *AGBL5*, post-translational modification

Retinitis pigmentosa (RP) (Mendelian Inheritance in Man [MIM]268000) encompasses a clinically and genetically heterogeneous group of inherited retinal dystrophies (IRDs) with a worldwide prevalence of approximately 1 in 4000 individuals. Retinitis pigmentosa is characterized by initial rod photoreceptor degeneration resulting in night blindness, followed by midperipheral visual field loss and deterioration of central vision due to cone photoreceptor degeneration.[1] The clinical presentation of RP is highly variable in terms of onset, disease progression, fundus appearance, and associated ocular features. The ophthalmic features indicative for RP include bone spicule pigmentations with atrophy of the retinal pigment epithelium (RPE), waxy disc pallor, and retinal arteriole attenuation.[2,3]

To date, 82 genes have been implicated in RP (https://sph.uth.edu/retnet; in the public domain). These genes encode proteins involved in different retinal pathways, including the phototransduction cascade, the retinoid cycle, ciliary transport,

Investigative Ophthalmology & Visual Science

retinal development, and RNA splicing factors.[4] Recent whole-exome sequencing (WES) studies demonstrated that approximately 60% of RP cases can be explained by variants in these genes (Haer-Wigman L, personal communication, 2016),[5–8] suggesting that several genes are yet to be identified. This study aimed to identify novel genes associated with RP using next-generation sequencing (NGS) technology.

Here, we describe the identification of biallelic variants in *AGBL5* in four autosomal recessive retinitis pigmentosa (arRP) patients from three unrelated families.

Subjects and Methods

Subjects and Clinical Evaluation

The study protocol adhered to the tenets of the Declaration of Helsinki and received approval from the respective local ethics committees. Written informed consent was obtained from all participants or parents of children prior to their inclusion in this study. Patients were ascertained from the inherited retinal disease clinics at the Rotterdam Eye Hospital (The Netherlands) and Moorfields Eye Hospital (London, UK).

Each patient underwent a full clinical examination including visual acuity and dilated fundus examination. Retinal fundus imaging was obtained by 35° color fundus photography (Topcon Great Britain Ltd, Berkshire, UK), 55° fundus autofluorescence (FAF) imaging (Spectralis; Heidelberg Engineering Ltd, Heidelberg, Germany), and Spectralis optical coherence tomography (OCT).

Full-field and pattern electroretinography (ERG, PERG) were available from three patients, performed with gold foil electrodes, which incorporated the International Society for Clinical Electrophysiology of Vision (ISCEV) standards.[9,10] We also studied all retrospective data including Stratus (Carl Zeiss Meditec, Dublin, CA, USA) OCTs.

Genetic Analysis

Genomic DNA was isolated from peripheral blood lymphocytes according to standard salting-out procedures.[11] In one unaffected individual from family 1, DNA was extracted from saliva material using the Oragene system (OG-500; Genotek, Ottawa, ON, Canada).

Whole-exome sequencing of the proband from family 1 was performed using Agilent's SureSelect All Human Exome version 2 kit (50 Mb; Agilent Technologies, Santa Clara, CA, USA), followed by sequencing on a SOLiD4 sequencing platform (Life Technologies, Carlsbad, CA, USA). Reads were mapped against the University of California, Santa Cruz (UCSC) genome browser, human Hg19 assembly (build 37) using Lifescope v2.1 software (Life Technologies), and variants were called using the Genome Analysis Toolkit (GATK) v2 according to the recommended guidelines (https://software.broadinstitute.org/gatk/best-practices/; in the public domain). Identified variants were filtered based on minor allele frequency < 0.005 in our internal cohort, and the Exome Aggregation Consortium (ExAC) database.

The proband from family 2 underwent WES analysis using Agilent's SureSelectXT Human All Exon version 5 exon capture (Agilent Technologies, Santa Clara, CA, USA), followed by sequencing on a HiSeq 2000 platform (Illumina, Inc., San Diego, CA, USA) at AROS Applied Biotechnology (Aarhus, Denmark). Raw fastq files were aligned to the GRCh37 reference genome using NovoAlign version 2.08.03 (Novocraft Technologies Sdn Bhd, Petaling Jaya, Selangor, Malaysia). Duplicate reads were marked using Picard tools MarkDuplicates (http://broadinstitute.github.io/picard; in the public domain). Calling was performed using the haplotype caller module of GATK (https://www.broadinstitute.org/gatk, version 3.3-0; in the public domain), creating gVCF formatted files for each sample. The individual gVCF files for the exomes discussed in this study, in combination with ~3000 clinical exomes (UCL-exomes consortium, University College London, London, UK), were combined into merged VCF files for each chromosome, on average containing 100 samples each. The final variant calling was performed using the GATK Genotype gVCFs module jointly for all samples (cases and controls). Variant quality scores were then recalibrated according to GATK best practices separately for indels and single nucleotide polymorphisms (SNPs). Resulting variants were annotated using ANNOVAR (http://annovar.openbioinformatics.org/; in the public domain) based on Ensembl (http://www.ensembl.org; in the public domain) gene and transcript definitions. Candidate variants were filtered based on function (non-synonymous, presumed loss of function or splicing, defined as intronic sites within 5 bp of an exon–intron junction) and minor allele frequency (<0.005 minor allele frequency in our internal control group, as well as the National Heart, Lung, and Blood Institute [NHLBI] exome sequencing dataset).

The patient from family 3 underwent whole-genome sequencing (WGS) as part of a large collaborative study: DNA from 599 unrelated patients with inherited retinal disease, ascertained from the Inherited Eye Disease clinics at Moorfields Eye Hospital (MEH), London, underwent WGS as part of the National Institute for Health Research England (NIHR) BioResource–Rare Diseases project, Specialist Pathology Evaluating Exomes in Diagnostics (SPEED). Briefly, peripheral blood mononuclear cell–derived genomic DNA was processed using the Illumina TruSeq DNA PCR-Free Sample Preparation kit (Illumina, Inc., San Diego, CA, USA) and sequenced using an Illumina HiSeq 2500, generating a minimum coverage of 15× for ~95% of the genome. Reads were aligned to the genome (GRCh37) using Isaac aligner (Illumina, Inc., Great Chesterford, UK). SNVs and indels were identified using Isaac variant caller. Variant examination was performed only on the single nucleotide variants (SNVs) and indels that met the following criteria: passed standard quality filters, predicted to alter the sequence of a protein, and had an allele frequency < 0.01 in the 1000 genomes database, the NHLBI GO Exome Sequencing Project (http://evs.gs.washington.edu/EVS/ release 20130513; in the public domain), the UK10K database (http://www.uk10k.org; in the public domain), the ExAC database (http://exac.broadinstitute.org; in the public domain), and allele frequency < 0.02 in ~6000 internal control genomes.

Sanger Sequencing

Primers for amplification of coding exons and flanking exon–intron boundaries of *AGBL5* (NM_021831.5) were designed with Primer3 plus (http://www.bioinformatics.nl/cgi-bin/primer3plus/primer3plus.cgi; in the public domain). Primer sequences and PCR conditions are available upon request.

Pathogenicity Interpretation of Missense Variant

The Combined Annotation Dependent Depletion (CADD) (http://cadd.gs.washington.edu/; in the public domain) score was used to predict the pathogenicity of missense variants. This scoring system incorporates several widely used in silico tools, such as SIFT (http://sift.jcvi.org/; in the public domain), PolyPhen-2 (http://genetics.bwh.harvard.edu/pph2/; in the public domain), Mutation Taster (http://www.mutationtaster.org/; in the public domain), PhyloP, and Grantham score. Minor allele frequencies were obtained from the Exome Aggregation Consortium (ExAC) database containing ~60,000 exomes of

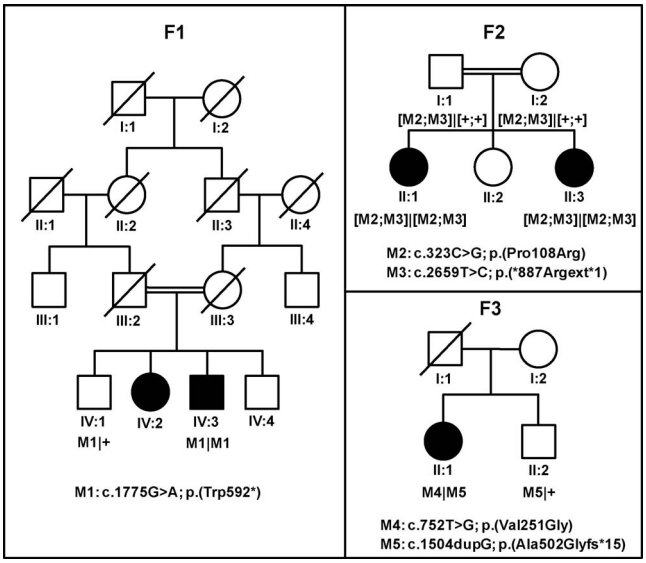

Figure 1. Pedigrees of families carrying *AGBL5* variants. *AGBL5* variants were identified in three autosomal recessive retinitis pigmentosa (RP) families. Affected individuals are indicated with *filled symbols* and unaffected relatives are indicated with *open symbols*. Genotypes are shown below the pedigree symbols. M represents mutant allele and '+' represents wild-type alleles. Variant c.1775G>A:p.(Trp592*) occurred in a homozygous state in F1; variants c.323C>G:p.(Pro108Arg) and c.2659T>C:p.(*887Argext*1) occurred in a homozygous manner in F2; and compound heterozygous variants c.752T>G:p.(Val251Gly) and c.1504dupG:p.(Ala502Glyfs*15) were found in F3.

unrelated individuals, accessed March 2016. YASARA (Yet Another Scientific Artificial Reality Application; http://www.yasara.org/; in the public domain) Structure molecular modeling package (Ver. 11.3.2) was used to build the three-dimensional structure of AGBL5 (AAH07415.2). Thereafter, two missense variants were introduced into this three-dimensional model to assess the predicted effect of these variants on the structure of the protein.

Results

Clinical Findings

The clinical characteristics of patients (for pedigrees, see Fig. 1) are summarized in Table 1, and retinal imaging pictures are shown in Figure 2. Patient F1-IV:3 was referred to the Rotterdam Eye Hospital at age 32 with end-stage RP complicated by cystoid maculopathy. Visual acuity at presentation was hand movements in the right and light perception in the left eye. He was pseudophakic (cataract extraction performed at age 29), and retrospective data on visual acuity and visual fields were not available. The cystoid maculopathy was responsive to subcutaneous octreotide, but visual acuity did not improve. Through the years the cysts disappeared and atrophy of the macular region developed (Figs. 2A, 2B). He was also suffering from Behcet's disease, but did not have a history of recurring uveitis. His older sister (F1-IV:2) was examined only once, at the age of 43. She also presented with end-stage RP. She was pseudophakic, and visual acuity was hand movement and counting fingers. Her fundus examination revealed optic disc pallor, attenuated vessels, macular atrophy, midperipheral and peripheral RPE atrophy, and heavy bone spicule pigmentation but no cystoid macular edema (not shown). The DNA sample of this patient was not available.

Patients from families 2 and 3 initially developed nyctalopia, with a range of onset from 9 to 30 years before subsequent development of peripheral visual field loss. At last review (age range, 24–45 years), there was mild visual acuity loss with best-corrected visual acuity mean 0.34 logMAR (range, 0.30–0.48). All patients developed posterior subcapsular cataract. Patient F2-II:1 had learning difficulties but no other symptoms suggestive of syndromic disease. There were fundus abnormalities consistent with RP including attenuated vessels, macular and midperipheral RPE mottling/atrophy, and peripheral intraretinal pigment migration, most prominent in the proband of family 3 (Fig. 2I). Fundus autofluorescence imaging demonstrated a ring of increased autofluorescence parafoveally in F2-II:1, focally increased autofluorescence corresponding to macular edema in F2-II:3, and a partial ring of reduced autofluorescence in F3-II:1 (Figs. 2D, 2G, 2J). All patients had midperipheral reduced autofluorescence in keeping with regions of RPE atrophy and increased pigmentation. On OCT, there was outer retinal atrophy with variable preservation of photoreceptors most apparent in F2-II:1 with a centrally preserved inner segment ellipsoid band (Fig. 2D). Optical coherence tomography imaging demonstrated intraretinal cysts of the inner nuclear layer, which responded to topical carbonic anhydrase inhibitors (Figs. 2E, 2H, 2K). Electrophysiology demonstrated rod and cone system dysfunction (Table 1).

Genetic Findings

Biallelic variants in *AGBL5* were identified in four patients from three families. These variants are summarized in Tables 1 and 2. None of them have been previously reported in RP patients. Whole-exome sequencing data analysis did not yield other biallelic variants in the genes known to be mutated in IRD (Retinal Information Network, https://sph.uth.edu/retnet/; in the public domain). The proband of family 1 was homozygous for the c.1775G>A:p.(Trp592*) nonsense variant in the *AGBL5* gene (Fig. 3). The resulting transcript is expected to undergo nonsense-mediated decay (NMD), suggesting that this variant is a true loss-of-function allele. This variant was reported in 1/121,398 alleles (0.0008%) in the ExAC dataset.

Two affected siblings from family 2 (GC15894) were homozygous for the missense variant c.323C>G:p.(Pro108Arg). All in silico tools predict this variant to be pathogenic (Table 2). The altered proline residue is fully conserved throughout AGBL5 orthologues up to *Tetraodon nigroviridis* (Fig. 3A) and is located in the core of AGBL5 (Fig. 3B). A change to arginine introduces a larger amino acid, which may destabilize the protein structure. Moreover, proline provides a rigid structure important for interaction with ligands or other proteins. A second homozygous variant, c.2659T>C:p.(*887Argext*1), was also identified in the two affected members of this family. This stop-loss variant is predicted to result in a single amino acid residue extension of the protein. Two rare stop-loss variants affecting other nucleotides of the *AGBL5* stop codon, c.2661A>G:p.(*887Trpext*1) and c.2661A>T:p.(*887Cysext*1), were found in one and seven alleles in the ExAC dataset, respectively.

The compound heterozygous variants c.1504dupG:p.(Ala502fs*15) and c.752T>G:p.(Val251Gly) were identified in a simplex RP patient of family 3. The p.(Val251Gly) variant alters the valine residue flanking the consensus zinc-binding residues of the M14-like peptidase domain. This valine is conserved throughout paralogues and orthologues of *AGBL5* (up to *T. nigroviridis*). Furthermore, it affects a highly conserved nucleotide with a PhyloP score of 4.73. According to Vissers et al.,[12] by using PhyloP score distribution of dbSNP and HGMD variants, this variant can be considered as

Table 1. Clinical Phenotype of Patients Carrying *AGBL5* Variants

Family ID, Sex, Origin	Variants		Age at Diagnosis, Recent Exam, y	History	Visual Acuity Snellen (logMAR)	Refraction	Ophthalmoscopy	Full Field ERG	OCT	FAF	Other Symptoms
	Allele 1	Allele 2									
F1–IV:3 (DNA12-19185), M, Turkey	c.1775G>A: p.(Trp592*)	c.1775G>A: p.(Trp592*)	16, 43	Central vision loss, nyctalopia (2nd decade)	RE: LP+ LE: LP−	NA (Pseudo-aphakia)	Mild optic disk pallor, attenuated vessels, macular and (mid-) peripheral RPE atrophy with heavy intraretinal bone spicule pigmentations and deep nummular pigmentations	NA	Cystoid maculopathy progressing into complete loss of outer retinal layers and thinning inner retinal layers at fovea	NP	Pseudophakia, cataract extraction (age 29), band keratopathy, cystoid macular edema (responsive to subcutaneous octreotide), Morbus Behçet
F2–II:1 (GC15894.1), F, UK	c.[323C>G; c.2659T>C]: p.[(Pro108Arg); (*887Argext*1)]	c.[323C>G; c.2659T>C]: p.[(Pro108Arg); (*887Argext*1)]	9, 24	Nyctalopia (age 9)	RE: 6/18 (0.48) LE: 6/12 (0.3)	RE: +0.50/−2.00 × 180 LE: −0.50/−1.50 × 170	Optic disc pallor, attenuated vessels, macular and midperipheral RPE mottling and occasional hyperpigmented spots	Age 8 y, findings of marked rod system dysfunction with cone system dysfunction R>L. Marked macular involvement on R	Cysts in inner nuclear layer L>R, centrally preserved inner segment ellipsoid band and outer nuclear layers L>R	Parafoveal hyper-autofluorescent ring larger on L, R additional ring of hypo-autofluorescence surrounding this in macula, midperipheral spots of hypo-autofluorescence	Posterior subcapsular cataract, cystoid macular edema (responsive to topical CAI), right amblyopia, right secondary exotropia
F2–II:3 (GC15894.2), F, UK	c.[323C>G; c.2659T>C]: p.[(Pro108Arg); (*887Argext*1)]	c.[323C>G; c.2659T>C]: p.[(Pro108Arg); (*887Argext*1)]	20, 27	Nyctalopia (2nd decade), central vision loss, visual field loss	RE: 6/18 (0.48) LE: 6/18 (0.48)	RE: −1.50/−2.50 × 48 LE: −1.50/−2.00 × 1	Optic disc pallor, attenuated vessels, macular and midperipheral RPE mottling, minimal pigment spots	Age 20 y, severe generalized loss of retinal function	Cysts inner nuclear layer, small foveal region of preserved inner segment ellipsoid band	Foveal hyper-autofluorescence surrounded by parafoveal hypo-autofluorescent ring, midperipheral spots of hypo-autofluorescence	Posterior subcapsular cataract, cystoid macular edema (responsive to CAI), learning difficulties
F3–II:1 (GC3687), F, UK	c.752T>G: p.(Val251Gly)	c.1504dupG: p.(Ala502-Glyfs*15)	39, 63	Nyctalopia, peripheral field loss, (start 4th decade)	RE: 6/12 (0.3) LE: 6/12 (0.3)	RE: 0/−1.00 × 65° LE: +0.25 DS	Optic disc pallor, attenuated vessels, macular RPE mottling, heavy midperipheral bone spicule pigmentation	Age 39 y, findings consistent with RP, report not available	Cysts in inner nuclear layer, centrally preserved outer nuclear layer and inner segment ellipsoid band (disrupted), epiretinal membrane	Parafoveal spots of hypo-autofluorescence, extensive speckled midperipheral loss of autofluorescence	Cataract, cystoid macular edema (responsive to CAI)

CAI, Carbonic Anhydrase Inhibitor; DS, Dioptres Sphere; FAF, fundus autofluorescence; L, left; LE, left eye; logMAR, Logarithm of the Minimum Angle of Resolution, to measure metric visual acuity; LP, light perception; NA, not applicable; NP, not performed; OCT, optical coherence tomography; R, right; RE, right eye; RPE, retinal pigmented epithelium.

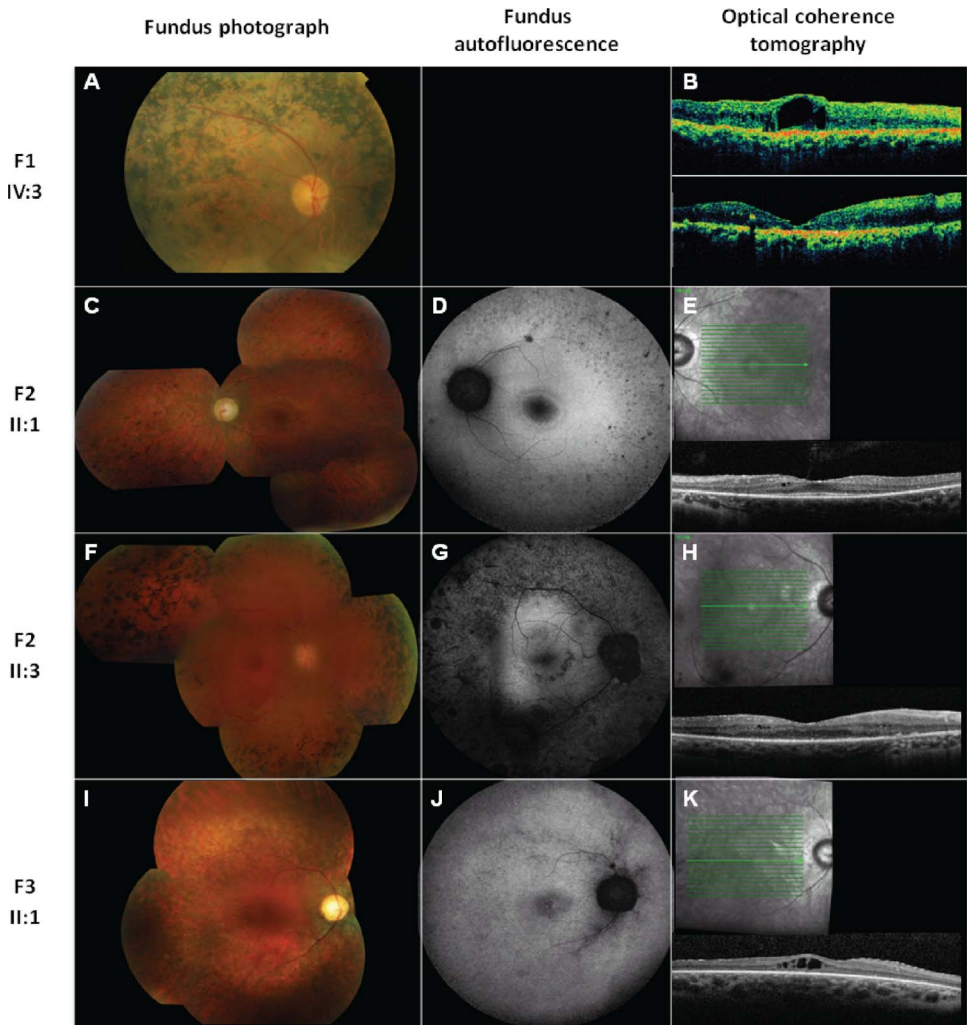

Figure 2. Retinal imaging of affected individuals. Color fundus imaging (**A**, **C**, **F**, **I**) in four patients demonstrated optic disc pallor, attenuated vessels, macular and midperipheral retinal pigment epithelium mottling/atrophy, and peripheral intraretinal pigment migration, heaviest in (**A**) and (**I**). FAF imaging in three patients demonstrated a ring of increased autofluorescence parafoveally in F2-II:1 (**D**) with focal parafoveal increased autofluorescence in F2-II:3 (**G**), likely representing cystoid macular edema. There was an incomplete ring of reduced autofluorescence parafoveally for F3-II:1 (**J**). All patients had midperipheral reduced autofluorescence in keeping with regions of RPE atrophy and increased pigmentation. Stratus OCT of the right eye in F1-IV:3 (**B**) at age 34 showed large cysts at the macula comprising several retinal layers with cysts in the inner nuclear layer of the paramacular region (*upper*). In the *lower* scan (at 39 years), complete atrophy of retinal layers at the fovea can be observed. OCT imaging also demonstrated loss of outer retina with partial preservation of the inner segment ellipsoid band in patient F2-II:1 (**E**), very limited photoreceptor preservation for F2-II.3 (**H**) and F3-II.1 (**K**), and intraretinal cysts of the inner nuclear layer for all patients.

pathogenic as it is close to the mean PhyloP score (4.7) of the pathogenic de novo variants identified in persons with intellectual disability. All in silico prediction tools indicate that this variant is pathogenic (Table 2). Alteration of this hydrophobic valine to glycine may destabilize the secondary structure of AGBL5 in this domain (Fig. 3B). All variants cosegregated with disease in the family members available for testing (Fig. 1).

Discussion

AGBL5 Is a Novel Gene Associated With RP

Previous studies by Patel et al.[5] and Kastner et al.[13] discovered *AGBL5* as a novel candidate gene associated with RP. These studies identified homozygous missense variants (p.(Arg276Trp) and p.(Asp295Asn)) in arRP cases from Saudi and Turkish origin.

Table 2. *AGBL5* Variants Identified in This Study and Their In Silico Analyses

DNA Variant	Protein Variant	ExAC Allele Frequency, %	SIFT	PolyPhen-2	Mutation Taster	CADD Phred	PhyloP
c.323C>G	p.(Pro108Arg)	0	Deleterious	Probably damaging	Disease causing	24.0	5.45
c.752T>G	p.(Val251Gly)	0	Deleterious	Probably damaging	Disease causing	27.1	4.73
c.1775G>A	p.(Trp592*)	0.0008	NA	NA	NA	NA	NA
c.1504dupG	p.(Ala502Glyfs*15)	0	NA	NA	NA	NA	NA
c.2659T>C	p.(*887Argext*1)	0	NA	NA	NA	NA	NA

NA, not applicable.

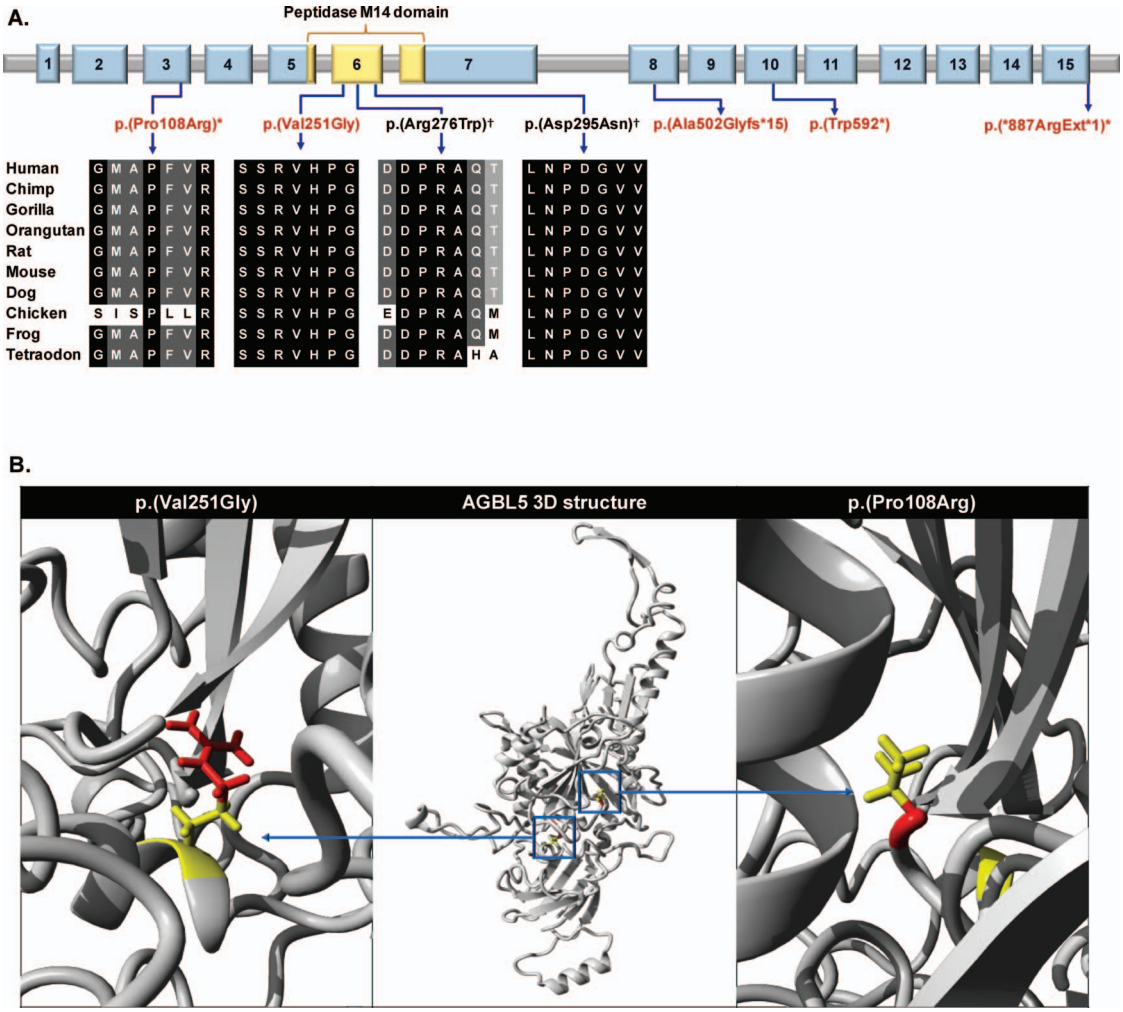

Figure 3. Exon–intron structure of *AGBL5*, RP-associated variants, and three-dimensional modeling of missense variants. (**A**) Schematic representation of *AGBL5* variants identified in this and previous studies. Cross-species amino acid comparison showed that all missense variants affect highly conserved residues. Variants identified in this study are colored in *red*, and variants in previous studies are in *black*. *These two variants occurred homozygously in F2. (**B**) Three-dimensional protein modeling of *AGBL5* missense variants. Three-dimensional structure of cytosolic carboxypeptidase-like protein 5; ATP/GTP-binding protein-like 5. Wild-type and mutant residues are shown and colored in *cyan* and *green*, respectively. The p.(Pro108Arg) variant, alter proline in position 108 to arginine, is located in the core of the AGBL5 protein. This alteration created a larger amino acid, which may destabilize the protein structure. The p.(Val251Gly) missense variant changed the hydrophobic valine to glycine and may destabilize the structure of *AGBL5*. †These two variants were identified from previous studies by Patel et al.[5] and Kastner et al.,[13] respectively.

In our study, we identified five novel variants in *AGBL5* in three unrelated RP cases that further confirm the causality of this gene. The novel variants consist of two missense, two protein-truncating, and one stop-loss variant. To date, all missense variants in *AGBL5* with the exception of p.(Pro108Arg) are located within the M14-like carboxypeptidase A domain (Fig. 3A), which highlights the importance of this protein domain for AGBL5 function. This protein domain encodes cytosolic carboxypeptidases (CCPs) that have been implicated to play a role in the posttranslational modifications of tubulin. Furthermore, mutation of the active site of the carboxypeptidase domain causes abnormal cilia development in zebrafish.[14] The protein-truncating variants, that is, p.(Trp592*) and p.(Ala502Glyfs*15), are expected to result in complete loss of function due to premature translation termination and NMD.

The stop-loss p.(*887Argext*1) variant found in family 2 results in loss of the canonical termination codon, which leads to the extension of the transcript by one codon and consequent extension of the protein by a single amino acid residue. This finding in addition to the presence of eight alleles in control data (ExAC) with similar stop-loss variants may suggest that the stop-loss variant is a bystander in the pathogenesis of *AGBL5* retinopathy, although a modifier or indeed pathogenic effect cannot be ruled out.

The two arRP families reported by Patel et al.[5] and Kastner et al.[13] display a classical RP phenotype, as do our patients. There was some variability in visual function; our eldest patient (age 63) still had relatively well-preserved visual acuity, whereas one subject was blind at age 32. All patients showed retinal cysts in the macula region at some stage of the disease, but this occurs in 18% to 32% of RP patients.[15]

Interestingly, Kastner et al.[13] reported intellectual disability in an affected male and proposed a possible correlation between sex and brain phenotype. In our study, learning difficulties occurred in a female patient, which does not support a correlation between sex and brain phenotypes. Additional RP patients with *AGBL5* variants need to be identified to gain more insight into a possible association with brain phenotypes.

Pathak et al.[14] demonstrated that knockdown of *Agbl5* in zebrafish leads to ciliopathy phenotypes, that is, axis curvature, hydrocephalus, pronephric cysts, and abnormal multicilia motility. However, in humans, variants in *AGBL5* are associated with nonsyndromic RP. These phenotypic discrepancies might be caused by homologous genes in humans that might compensate for the effect caused by these mutations. Alternatively, as the NMD event was not functionally assessed, there is a possibility that in the human patients, truncated proteins with residual activity are being produced. Finally, recent studies show that the use of morpholinos for gene knockdown in zebrafish may lead to off-target effects, thereby explaining additional phenotypes observed in the zebrafish studies.[16]

Imbalance of Poly- and Deglutamylation in Posttranslational Modifications Is Associated With RP

Approximately one-third of IRD-associated genes play roles in maintaining the structure and function of photoreceptor sensory cilium.[17] Previous studies have implicated *TTLL5*, a gene encoding a polyglutamylase (tubulin tyrosine ligase-like family, member 5) in the pathogenesis of autosomal recessive cone–rod dystrophy.[18] *AGBL5*, also known as *CCP5*, is known to function in polyglutamylation and deglutamylation of tubulin, and perturbations in this pathway may lead to photoreceptor cell degeneration.[19] Tubulin glutamylation is an essential posttranslational modification associated with stable microtubules, neuronal axons, mitotic spindles, centrioles, and cilia.[20] The tubulin tyrosine ligase-like (TTLL) and CCP deglutamylases are required to maintain the balance of tubulin glutamylation in ciliogenesis.[21,22] Any imbalance in poly- and deglutamylation might disrupt cilia function. Hyperglutamylation is known to diminish *Tetrahymena* cilia motility and to induce axonemal microtubules defects.[23] *Ttll5* mutant mice displayed a complete loss of retinitis pigmentosa GTPase regulator (RPGR) glutamylation without marked changes in tubulin glutamylation levels. The *Ttll5* mutant mouse developed slow photoreceptor degeneration with early mislocalization of cone opsins, features resembling those of *Rpgr*-null mice.[18] *Ccp5* knockdown in zebrafish led to hyperglutamylation and reduced the disorganized cilia beat pattern. Ttll5, on the other hand, plays a role in polyglutamylation, which is crucial for microtubule sliding and cilia waveform regulation.[15] Interestingly, a recent study demonstrates the role of *TTLL5* in *RPGR*^{ORF15} glutamylation.[24] The opposite function of AGBL5 (CCP5) in the deglutamylation process may also play an important role in the balance of glutamate chains in RPGR^{ORF15}. Posttranslational modifications are regulated by several members of the *TTLL* and *CCP* gene families, and we hypothesize that besides *AGBL5* and *TTLL5*, other *TTLL* (*TTLL1* through *TTLL11*) and *CCP* (*CCP1* through *CCP6*) genes are plausible candidate genes for IRD.

In conclusion, this study strengthens the role of *AGBL5* variants in RP. The involvement of both *AGBL5* and *TTLL5* in IRDs underlines the critical importance of glutamylation in retinal function.

Acknowledgments

The authors thank the patients and family members for participation in the study.

The research of GDNA was supported by the Directorate General for Higher Education (DIKTI) of the Ministry for National Education of Indonesia and the Radboud University Medical Center, Nijmegen, The Netherlands. The research of GA, SH, and ARW was supported by the National Institute for Health Research England (NIHR) BioResource–Rare Diseases (RG65966), the NIHR Biomedical Research Centre at Moorfields Eye Hospital, and the University College London Institute of Ophthalmology (BRC2_003); the Foundation Fighting Blindness (USA, C-CL:0710-0505-MEH10-02); Fight For Sight (1318 and 1801); Moorfields Eye Hospital Special Trustees (ST1109B); Rosetrees Trust (M184); RP Fighting Blindness (GR581). LP is supported by Foundation Combined Ophthalmic Research Rotterdam (CORR).

Disclosure: **G.D.N. Astuti**, None; **G. Arno**, None; **S. Hull**, None; **L. Pierrache**, None; **H. Venselaar**, None; **K. Carss,** None; **F.L. Raymond**, None; **R.W.J. Collin**, None; **S.M.H. Faradz**, None; **L.I. van den Born**, None; **A.R. Webster**, None; **F.P.M. Cremers**, None

References

1. Hamel C. Retinitis pigmentosa. *Orphanet J Rare Dis*. 2006;1:40.
2. Weleber R, Gregory-Evans K. Retinitis pigmentosa and allied disorders. In: Ryan SJ, ed. *Retina*. St. Louis: Mosby; 2001:362–470.
3. Friedenwald J. Discussion of Verhoeff's observations of pathology of retinitis pigmentosa. *Arch Ophthalmol*. 1930;767–770.
4. den Hollander AI, Black A, Bennett J, Cremers FP. Lighting a candle in the dark: advances in genetics and gene therapy of recessive retinal dystrophies. *J Clin Invest*. 2010;120:3042–3053.
5. Patel N, Aldahmesh MA, Alkuraya H, et al. Expanding the clinical, allelic, and locus heterogeneity of retinal dystrophies. *Genet Med*. 2016;18:554–562.
6. Abu-Safieh L, Alrashed M, Anazi S, et al. Autozygome-guided exome sequencing in retinal dystrophy patients reveals pathogenetic mutations and novel candidate disease genes. *Genome Res*. 2013;23:236–247.
7. Beryozkin A, Shevah E, Kimchi A, et al. Whole exome sequencing reveals mutations in known retinal disease genes in 33 out of 68 Israeli families with inherited retinopathies. *Sci Rep*. 2015;5:13187.
8. Weisschuh N, Mayer AK, Strom TM, et al. Mutation detection in patients with retinal dystrophies using targeted next generation sequencing. *PLoS One*. 2016;11:e0145951.
9. Bach M, Brigell MG, Hawlina M, et al. ISCEV standard for clinical pattern electroretinography (PERG): 2012 update. *Doc Ophthalmol*. 2013;126:1–7.
10. McCulloch DL, Marmor MF, Brigell MG, et al. ISCEV Standard for full-field clinical electroretinography (2015 update). *Doc Ophthalmol*. 2015;130:1–12.
11. Miller SA, Dykes DD, Polesky HF. A simple salting out procedure for extracting DNA from human nucleated cells. *Nucleic Acids Res*. 1988;16:1215.
12. Vissers LE, de Ligt J, Gilissen C, et al. A de novo paradigm for mental retardation. *Nat Genet*. 2010;42:1109–1112.
13. Kastner S, Thiemann IJ, Dekomien G, et al. Exome sequencing reveals *AGBL5* as novel candidate gene and additional variants for retinitis pigmentosa in five Turkish families. *Invest Ophthalmol Vis Sci*. 2015;56:8045–8053.
14. Pathak N, Austin-Tse CA, Liu Y, Vasilyev A, Drummond IA. Cytoplasmic carboxypeptidase 5 regulates tubulin glutamylation and zebrafish cilia formation and function. *Mol Biol Cell*. 2014;25:1836–1844.
15. Hajali M, Fishman GA. The prevalence of cystoid macular oedema on optical coherence tomography in retinitis pigmentosa patients without cystic changes on fundus examination. *Eye (Lond)*. 2009;23:915–919.
16. Bedell VM, Westcot SE, Ekker SC. Lessons from morpholino-based screening in zebrafish. *Brief Funct Genomics*. 2011;10:181–188.

17. Estrada-Cuzcano A, Roepman R, Cremers FP, den Hollander AI, Mans DA. Non-syndromic retinal ciliopathies: translating gene discovery into therapy. *Hum Mol Genet*. 2012;21:R111–R124.
18. Sergouniotis PI, Chakarova C, Murphy C, et al. Biallelic variants in *TTLL5*, encoding a tubulin glutamylase cause retinal dystrophy. *Am J Hum Genet*. 2014;94:760–769.
19. Yu I, Garnham CP, Roll-Mecak A. Writing and reading the tubulin code. *J Biol Chem*. 2015;290:17163–17172.
20. Edde B, Rossier J, Le Caer JP, Desbruyeres E, Gros F, Denoulet P. Posttranslational glutamylation of alpha-tubulin. *Science*. 1990; 247:83–85.
21. Rogowski K, van Dijk J, Magiera MM, et al. A family of protein-deglutamylating enzymes associated with neurodegeneration. *Cell*. 2010;143:564–578.
22. van Dijk J, Rogowski K, Miro J, Lacroix B, Edde B, Janke C. A targeted multienzyme mechanism for selective microtubule polyglutamylation. *Mol Cell*. 2007;26:437–448.
23. Janke C, Rogowski K, Wloga D, et al. Tubulin polyglutamylase enzymes are members of the TTL domain protein family. *Science*. 2005;308:1758–1762.
24. Sun X, Park JH, Gumerson J, et al. Loss of *RPGR* glutamylation underlies the pathogenic mechanism of retinal dystrophy caused by *TTLL5* mutations. *Proc Natl Acad Sci U S A*. 2016; 113:E2925–E2934.